Solid State Phenomena
ISSN: 1662-9779, Vol. 389, pp 253-266
doi:10.4028/p-gAD5RR

Submitted: 2026-01-19
Revised: 2026-02-22
Accepted: 2026-02-24
Online: 2026-04-16

Reducing the Uncertainty in Flow Forming of Metastable Austenites

Lukas Kersting[1,a,*], Mustafa Koyuncu[1], Bahman Arian[2, b], Julian Rozo Vasquez[3,c], Ansgar Trächtler[1,4,d], Werner Homberg[2,e] and Frank Walther[3,f]

[1]Fraunhofer Institute for Mechatronic Systems Design (IEM), Paderborn, Germany

[2]Paderborn University, Forming and Machining Technology (LUF), Germany

[3]TU Dortmund University, Chair of Materials Test Engineering (WPT), Germany

[4]Heinz Nixdorf Institute (HNI), Paderborn University, Germany

[a]lukas.kersting@iem.fraunhofer.de; [b]ba@luf.uni-paderborn.de; [c]julian.rozo@tu-dortmund.de; [d]ansgar.traechtler@hni.uni-paderborn.de; [e]wh@luf.uni-paderborn.de; [f]frank.walther@tu-dortmund.de
*corresponding author

Keywords: Flow forming, metastable austenites, uncertainty, closed-loop property control

Abstract. Flow forming of metastable austenites is an innovative, incremental metal forming process with special capabilities due to the TRIP effect. However, the TRIP effect during flow forming is significantly affected by disturbances and especially batch fluctuations leading to process uncertainty. This aspect is further analyzed and quantified in this paper to give insights on how to minimize the impact of uncertainty. For this purpose, semifinished parts and resulting flow forming workpieces are systemically characterized concerning their properties and the property uncertainty supported by mathematical methods like correlation analysis and error propagation. A result is that the most influencing impact factor on the strain induced α'-martensite volume fraction as a material property are batch fluctuations, specifically the variations of the chemical composition. Those especially appear from batch to batch, but also within a batch accompanied by e.g. temperature effects. To counter this challenge, different methods from control theory like closed-loop property control and adaptive control can be applied to flow forming. Thus, uncertainty will be reduced to increase process robustness and to enable industrial exploitation of the TRIP effect in flow forming of metastable austenitic steels.

Introduction

In the automotive, aerospace and railway industry, there is a rising demand on high strength, lightweight and tamper-proof metal forming parts [1]. In context of tubular parts, flow forming of metastable austenites is proposed in academic literature as a suitable, innovative metal forming process for manufacturing [2–4]. Here, locally restricted areas of α'-martensite can be integrated into an austenitic semifinished part that might act as an invisible magnetic or QR code or as wear resistant functional elements since α'-martensite has a higher hardness and is ferromagnetic in contrast to austenite which is paramagnetic. To form the α'-martensite in the austenitic semifinished part, the TRIP effect (Transformation Induced Plasticity) of metastable austenites like AISI 304 / AISI 304L is used. Here, a strain-induced phase transformation from γ-austenite to α'-martensite takes place during plastic deformation. However besides plastic deformation and the effect of factors such as grain size and strain rate, the phase transformation is especially influenced by the forming temperature and the chemical composition of the material [5]. For this reason, the TRIP effect during metal forming is often considered as difficult to reproduce. Distinct applications are primarily found in academic literature e.g. for flow forming, deep drawing or bulk metal forming (c.f. [6–8]). In industrial mass production however, even if AISI 304 is a wide-spread material, the TRIP effect depicts more a challenge than a useful feature [9]. Taking a special regard to the flow forming process, no industrial application is known where the TRIP effect is specifically used to set the workpiece properties. This might also be due to flow forming's process complexity. That means flow forming has many process parameters that interact in a complex way with the measurable properties of the manufactured workpieces such as the geometry or α'-martensite volume faction. However, some of the input parameters such as the geometry and material properties of the semifinished parts fluctuate, e.g. due to the accuracy and tolerances of upstream manufacturing processes [10]. Additional disturbances are also possible during the manufacturing like temperature effects. Those factors leads to a certain uncertainty in flow forming that affect the product quality [10]. There are generally different types of uncertainty in literature. It can be distinguished between aleatoric uncertainty like stochastic effects and epistemic uncertainty due to a lack of knowledge. The term uncertainty is also connected to the uncertainty of the quality measurement and of prediction models. Fortunately, it is possible to overcome uncertainty if it can be described and evaluated [11]. However, even if there are some publications that mention the uncertainty in flow forming (and also separately for the TRIP effect), there is to our knowledge no quantitative study that describes and evaluates uncertainty in flow forming of metastable austenites. This paper tries to fill the gap by presenting an experimental study about the uncertainty in flow forming of metastable austenites. In the following, uncertainty is characterized and mathematically evaluated based on experimental data from different material batches, accompanying the whole chain from the semifinished part to the final workpiece. When uncertainty is known, it will be shown and discussed how current research from the field of control engineering can help to master the uncertainty in flow forming of metastable austenites and thus improve the manufacturing process.

Process, Setup and Background

Process setup. In context of this paper, flow forming of metastable austenites especially focusses on backward flow forming with a single roller flow forming machine. Here, a roller tool is axially moved with a defined radial infeed Δr and axial feed rate $f = \dot{x}_{\text{roller}}$ alongside a rotating workpiece (see Fig. 1a). This leads to characteristic plastic deformation of the material below the roller. In consequence, there is a wall thickness reduction Δw of the initial wall thickness w_0, a material flow in opposite direction to the roller motion leading an elongation of the initial length L_0 by ΔL and also a change of the α'-martensite volume fraction of the metastable austenitic workpiece material due to the strain induced phase transformation. However, the actual amount of martensite formation, elongation and wall thickness reduction also depends on the semifinished parts with its initial properties and uncertainties.

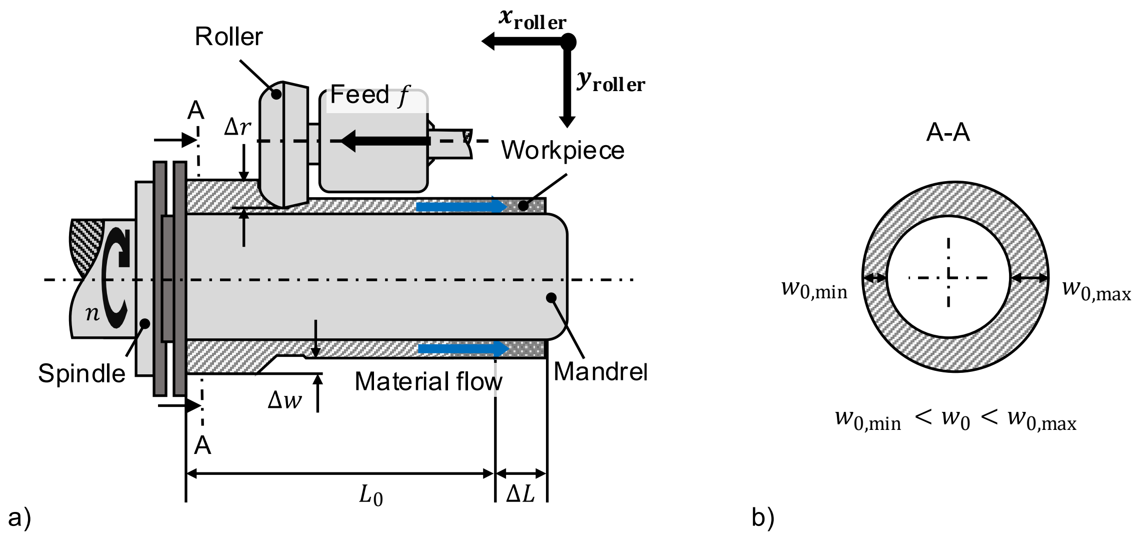

Fig. 1. Backward flow forming process (a) and eccentricity of the semifinished parts (b)

Semifinished parts and material. In this paper, tubular semifinished parts from AISI 304L (DIN 1.4307, X2CrNi18-9) are used. The material is a stainless, metastable austenitic Cr-Ni-steel which is nominally pure austenitic. It contains austenite stabilizing alloying elements like carbon (C), manganese (Mn), or nitrogen (Ni) and elements that support martensite formation during plastic deformation like silicon (Si) or chrome (Cr) [19]. The chemical composition, as defined by DIN EN 10216-5, is given by Table 1.

Table 1. Chemical composition of AISI 304L (1.4307, X2CrNi18-9) according to DIN EN 10216-5 [12] and the manufacturer data sheet for different batches of semifinished parts

	C	Si	Mn	P	S	N	Cr	Ni
DIN 10216-5	≤ 0.030	≤ 1.00	≤ 2.00	≤ 0.040	≤ 0.015	≤ 0.10	17.5 – 19.5	8.0 – 10.0
Batch A	0.019 – 0.021	0.25 – 0.27	1.12 – 1.13	0.030 – 0.031	0.002 – 0.006	0.07	18.3	8.2
Batch B	0.021 – 0.022	0.35 – 0.38	1.87 – 1.89	0.035 – 0.036	0.006 – 0.007	0.09	18.2	8.1
Batch C	0.018 – 0.022	0.31 – 0.37	1.26 – 1.78	0.032 – 0.036	0.003 – 0.013	0.03 – 0.10	18.2 – 18.4	8.1 – 8.2
Batch D	0.020	0.39	1.62	0.038	0.002	0.03	18.4	9.2
Batch E	0.020 – 0.021	0.26 – 0.28	1.35 – 1.38	0.032 – 0.036	0.006 – 0.008	0.06	18.3 – 18.4	8.2 – 8.3

However, the norm only defines boundaries for the chemical conditions. Thus, the actual chemical composition might differ from batch to batch due to tolerances. To illustrate this effect, Table 1 also contains the actual composition of five different material batches according to the manufacturer data sheets that were available to the authors of this paper. Except for Batch D, each data sheet contains the results of multiple samples that vary within a batch. It has also to be noted that the amount of some chemical elements such as copper, molybdenum or niobium is not defined in the norm. The fraction of those elements is oftentimes not delivered by the data sheet and remain uncertain since they are not controlled by the manufacturer. The semifinished parts used in this paper are cold drawn, seamless tubes manufactured according to DIN EN 1016-5. The tubes have an external diameter $d =$ 80 mm, initial wall thickness $w_0 = 4$ mm and initial length $L_0 = 150$ mm. However, the initial wall thickness w_0 can vary up to ± 10 % and the external diameter up to ± 0,75 % according to the norm [12]. Thus, those parameters also include uncertainty due to the variation. It has to be noted that the variation can appear from part-to-part and in a single part by the tube eccentricity (see Fig. 1b). This effect is analyzed in Fig. 2. Here, the initial wall thickness w_0 was determined for a total of 144 semifinished parts from the five material batches at 24 measuring points axially and angularly distributed alongside the shape. The measurements were manually performed with caliper D4R50 (Kroeplin, Schluechtern). The results show that the mean initial wall thickness of the investigated batches, characterized by the median in the boxplots of Fig. 2, varies from 3.9 mm to 4.26 mm and also within a batch, the mean initial wall thickness w_0 of each part vary up to 0.3 mm. Thus, there is a total variation of mean w_0 between 3.75 mm (lowest value Batch B) and 4.4 mm (highest value Batch A) with certain overlap between the batches near the nominal value of 4 mm. Each value is within the tolerances given by DIN EN 1016-5, but the permissible range is almost entirely covered due to the variance in the reality.

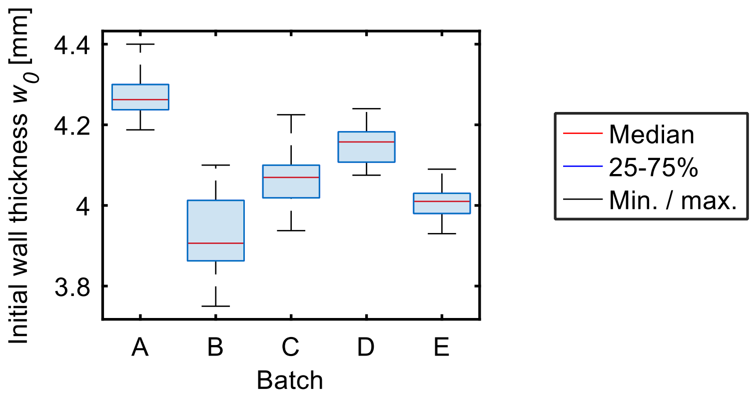

Fig. 2. Uncertainty of the (mean) initial wall thickness w_0 from semifinished part to semifinished part for different material batches

In contrast to the tolerated variance of w_0, the initial α'-martensite volume fraction α'_0 of the semifinished parts from AISI 304L is nominally defined to be zero. However, measurements with Feritscope FMP30 (Fischer, Sindelfingen) have shown that also a slight variation of up to 1 Vol.-% can be detected in reality that might be due to the undesired inclusion of ferromagnetic phases or the presence of conductive elements such as copper. This effect also varies from batch to batch and from part to part as an uncertainty (see Fig. 3).

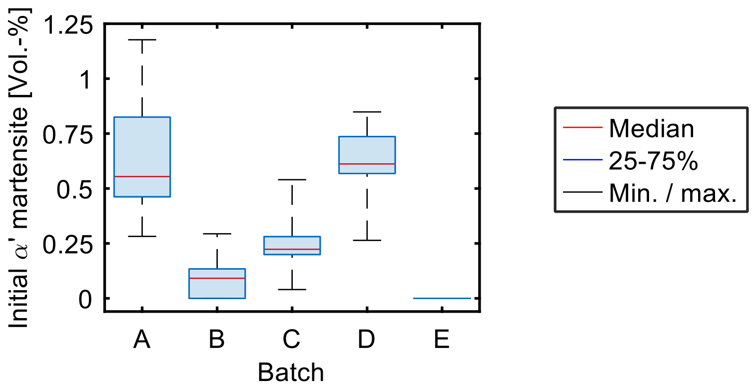

Fig. 3. Uncertainty of the (mean) initial α'-martensite volume fraction α'_0

It can be concluded that from the semifinished parts result a certain uncertainty that might affect the flow forming process, as will be investigated in the following of this paper. However, also the measurements have a certain uncertainty due to the limited accuracy of the measurement devices used for characterization.

Measurement devices for materials characterization. In this paper, caliper D4R50 is used for measurement of the wall thickness or the determination of the wall thickness reduction Δw with an accuracy of approx. ± 0,05 mm. The α'-martensite volume fraction is determined in this paper by nondestructive material testing. Here, the measurements are performed by Feritscope FMP30, that utilizes the magneto-inductive method as working principle and the correlation for the α'-martensite calculation by Talonen et al. [13]. The overall accuracy for the configuration used in this paper is 3 % at maximum according to the manufacturer.

Procedure

Methodology. The impact of the previously described uncertainty of the semifinished parts on the final flow forming workpiece is further analyzed and quantified in the following, taking the example of two different material batches (Batch A and Batch B). For this purpose, a full factorial series of experimental investigations was performed to characterize Batch B using a single roller flow forming machine Leifeld PLB 400 from Paderborn University (see [14, 15] for further details on the machine). In the experiments, workpieces were manufactured using 9 different process parameter combinations, i.e. the feed rate f (0.1 mm/s, 0.3 mm/s, 0.5 mm/s) and the infeed Δr (1 mm, 2 mm, 3 mm) varied from workpiece to workpiece, while the rotational speed remained constant at 30 rpm. The experiments were conducted under isothermal conditions due to the cooling from the machine. However, insufficient cooling might be a disturbance variable that affects the results. Thus, the ambient and cooling temperature were also monitored among others during the experiments to capture this source of uncertainty. To handle the uncertainty, each experiment was conducted twice, as frequently performed in the flow forming literature for statistical reasons (see e.g. [16]). The results were supplemented by previous experiments that were performed under the same conditions (machine, characterization methods) in the past for Batch A. Those results were already published in [17] and will be compared to the new results for Batch B in the following. At first, the overall transfer behavior of each batch is identified which is characterized by the mean value of wall thickness reduction Δw and α'-martensite volume fraction of each specimen or process parameter combination. Based on this, the uncertainty within a batch is determined and compared to the batch-to-batch variation of the transfer behavior. The results are further discussed in the following.

Analysis of the transfer behavior (Uncertainty from batch to batch). For the analysis of the overall transfer behavior of each batch, the mean wall thickness reduction Δw of each workpiece is plotted against the process parameters f and Δr (see Fig. 4). It can be seen that Δw arise by reducing the feed and increasing the infeed. This effect is in accordance to the literature [18] and should not be further discussed at this point. Here, the focus is quantitively on the batch dependency. According to the figure, the mean wall thickness reduction Δw for both batches is quantitatively in the same range. In the experiments of Batch B, Δw tends to be larger than in Batch A. However, the mean deviation between both batches is only 0.03 mm which is in the range of the measurement accuracy of the caliper and might also result from small differences in the experimental conditions in both experimental series (e.g. operator of the machine and measurement device). Thus, it can be concluded that there is only a minor batch dependency of the resulting wall thickness reduction Δw.

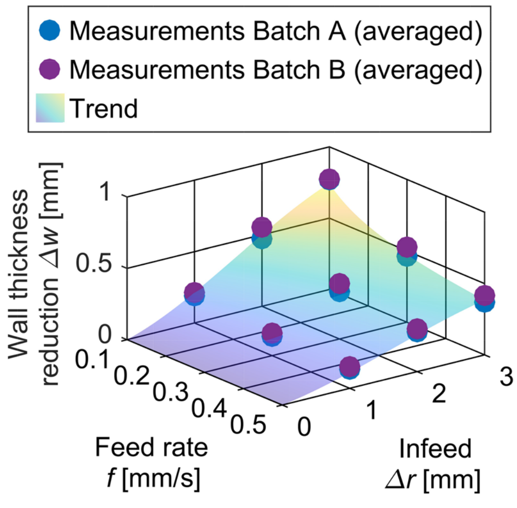

Fig. 4. Transfer behavior of the wall thickness reduction Δw for Batch A and B

For the analysis of the overall transfer behavior of the α'-martensite formation, the α'-martensite volume fraction of each workpiece is measured using the Feritscope FMP30. From the literature, it is already known that measurements should correlate in a sigmoidal shape to the strain [19, 20]. In flow forming there is especially a dependency on the radial strain φ_r, that corresponds to the wall thickness reduction by Eq. 1

$$\varphi_r = \ln \frac{w_0 - \Delta w}{w_0}, \tag{1}$$

and the feed rate f as already found by Riepold et al. [21]. Thus, the results are plotted for the batch analysis against f and φ_r which is calculated by Eq. 1 from the measurements of Δw.

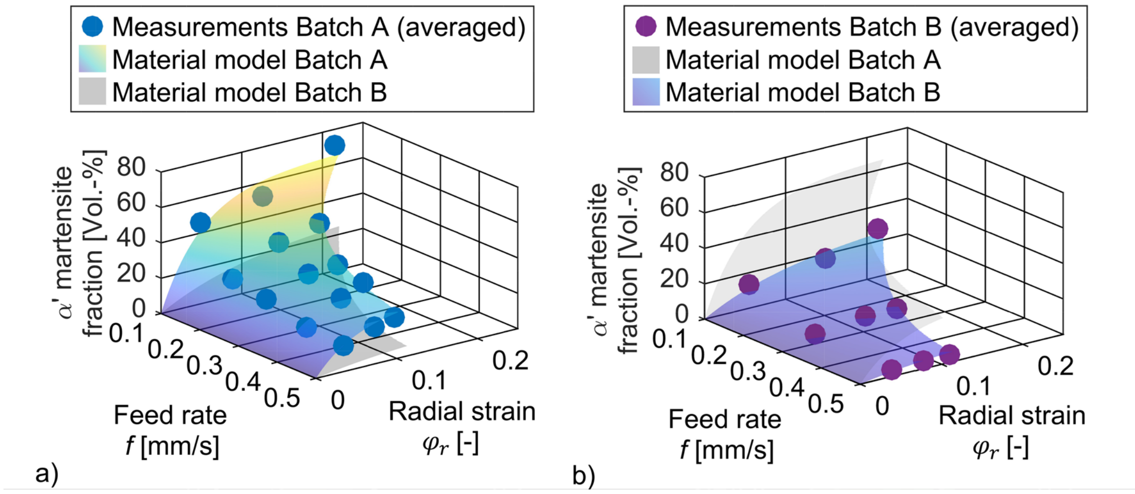

Fig. 5. Transfer behavior of the α'-martensite fraction for Batch A (a) and Batch B (b)

It can be seen from Fig. 5 that in both batches the α'-martensite volume fraction arises by reducing feed rate f and increasing φ_r which is conform to the literature (see [21]). However, the results quantitively deviate from batch to batch. For Batch A, the maximum value is 71 Vol.-%, but in Batch B only 27 Vol.-% of α'-martensite is induced for the same feed rate f and a similar radial strain φ_r. This also applies to the other measurement results. Thus, a clear dependency on the batches can be stated because both experimental series were performed under the same nominal boundary conditions (machine, cooling temperature). It might be caused by the higher amount of austenite stabilizing manganese (Mn) and nitrogen (N) in Batch B according to Table 1 and probably by austenite stabilizing elements that are not defined in the data sheet such as copper.

To deeper analyze and to characterize the effect of the different batches on the overall transfer behavior, the measurements were approximated by a material model function (see color and grey surfaces in Fig. 5). Here, an approach from [21] for three roller flow forming has already been adapted to single roller flow forming in previous investigations by the authors. This leads to Eq. 2:

$$\alpha' = g_\alpha(\Delta w, f) = c_1 \cdot \left(1 - \exp\left(-\text{abs}\left(\frac{\varphi_r(\Delta w)}{c_2}\right)\right)\right) \cdot \left(f^{-c_3}\right). \quad (2)$$

In the equation, the first term represents the dependency on radial strain φ_r. It resembles the models of Smaga et al. [22] or Olson and Cohen [20] that describe the nucleation and growth of α'-martensite by a sigmoidal function. The first term thus could be interpreted as a phenomenological component of the equation. In the second term, the dependency on feed rate during flow forming is described by an exponential function as an ansatz function to approximate the data. In the equation, the parameters c_1, c_2 and c_3 are regression coefficients that can be determined by nonlinear regression (see [17, 21]). The parameters of Batch A were already determined in the previous investigations by the authors and are shown in Table 2.

Table 2. Material model parameters

	c_1	c_2	c_3
Batch A	19.872	0.0445	0.5169
Batch B	5.0599	0.1041	0.7425

The table also includes the parameters for Batch B that are newly identified by nonlinear regression. In both cases, the deviations between Eq. 2 and the measurement data are less than 5 Vol.-% with two exceptions at all (see Fig. 6). Thus, it can be concluded that the general functional relationship between the feed rate f, radial strain φ_r and α'-martensite volume fraction is the same, but the parameters vary depending on the batch. This is an important gain in knowledge given by the experimental study in this paper. It shows that the previously investigated material model approach for flow forming is transferable to other material batches and that the batch-to-batch variation of the transfer behavior can be characterized as a variation of the model parameters.

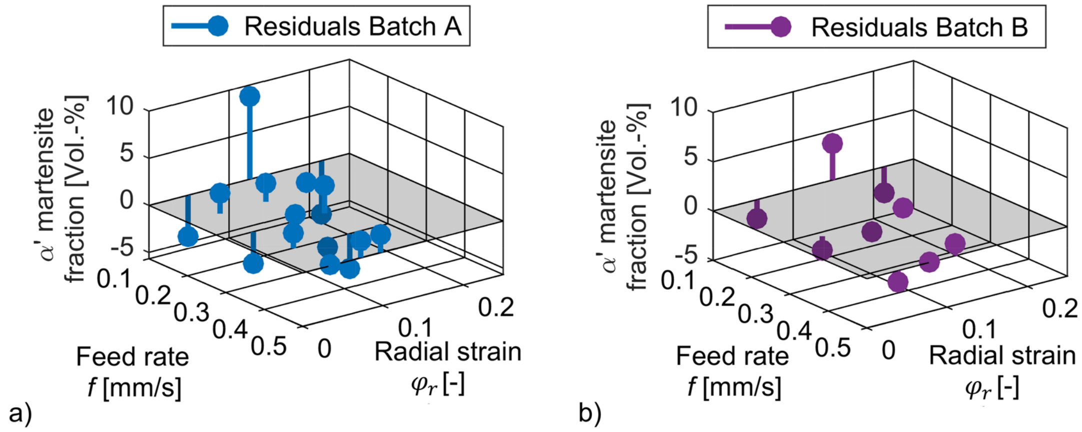

Fig. 6. Residuals between material model and measurements for Batch A (a) and Batch B (b)

This batch-to-batch variation depicts an important uncertainty concerning the α'-martensite formation in flow forming of metastable austenites. However, there are also variations within a batch that are not visible when analyzing only the average α'-martensite volume fraction or the average wall thickness reduction. For this purpose, it is necessary to analyze the wall thickness and the α'-martensite volume fraction of every individual workpiece on its own. Thus, the uncertainty from workpiece to workpiece within the batch can be characterized. The results will be discussed in the following.

Characterization of uncertainty within a batch. To characterize the uncertainty within a batch, the deviation of single measurement values from the average for each process parameter combination, i.e. the deviation from the transfer behavior, is further analyzed. For the wall thickness reduction Δw of Batch A, it can be seen from Fig. 7a that the measurement values deviate between -0.03 mm and 0.04 mm from the average value. However, for most process parameter combinations the deviation is lower. Thus, the mean deviation of all process parameter combinations is 0.014 mm. For Batch B, the results are similar (see Fig. 7b). Here, the deviation lays in a range between -0.05 mm and 0.05 mm, and the mean deviation is 0.02 mm. Hence, there is no batch dependency on the results. Furthermore, there is no clear dependency on process parameters visible for both batches. Thus, the deviation seems to be a stochastic effect. The amount of deviation is in the range of the measurement accuracy of the caliper D4R50 that was utilized for the wall thickness measurement. For this reason, it cannot be clearly stated whether the deviation results from the measurement, from inhomogeneities of the initial wall thickness within a batch or from other random effects.

For the α'-martensite volume fraction of Batch A, the results are shown in Fig. 7c. Here, the measurement values by Feritscope FMP30 deviate -4.36 Vol.-% and 3.6 Vol.-% from the average value and the mean deviation is 1.96 Vol-%. For Batch B, the deviation is much lower with range of ±1.165 Vol.-% and a mean deviation of 0.425 Vol.-% (see Fig. 7d). Thus, a clear batch dependency on the uncertainty is obvious that correlates to the amount of α'-martensite. For example, the mean percentage deviation (quotient of deviation and average value) is 7 % for Batch A and 5 % for Batch B with a maximum deviation of 18 % for Batch A and 19 % for Batch B. This percentage deviation exceeds the measurement error of the Feritscope that has a trueness error of ≤ 3 % and a repeatability error of ≤ 1 % according to the data sheet of the manufacturer. Thus, other possible reasons are analyzed based on the material model (Eq. 2).

Batch A			
Max. $\lvert\delta\Delta w\rvert$	0.04 mm	Max. $\lvert\delta\alpha'\rvert$	4.4 Vol.-%
Mean $\lvert\delta\Delta w\rvert$	0.01 mm	Mean $\lvert\delta\alpha'\rvert$	2.0 Vol.-%

Batch B			
Max. $\lvert\delta\Delta w\rvert$	0.05 mm	Max. $\lvert\delta\alpha'\rvert$	1.7 Vol.-%
Mean $\lvert\delta\Delta w\rvert$	0.02 mm	Mean $\lvert\delta\alpha'\rvert$	0.4 Vol.-%

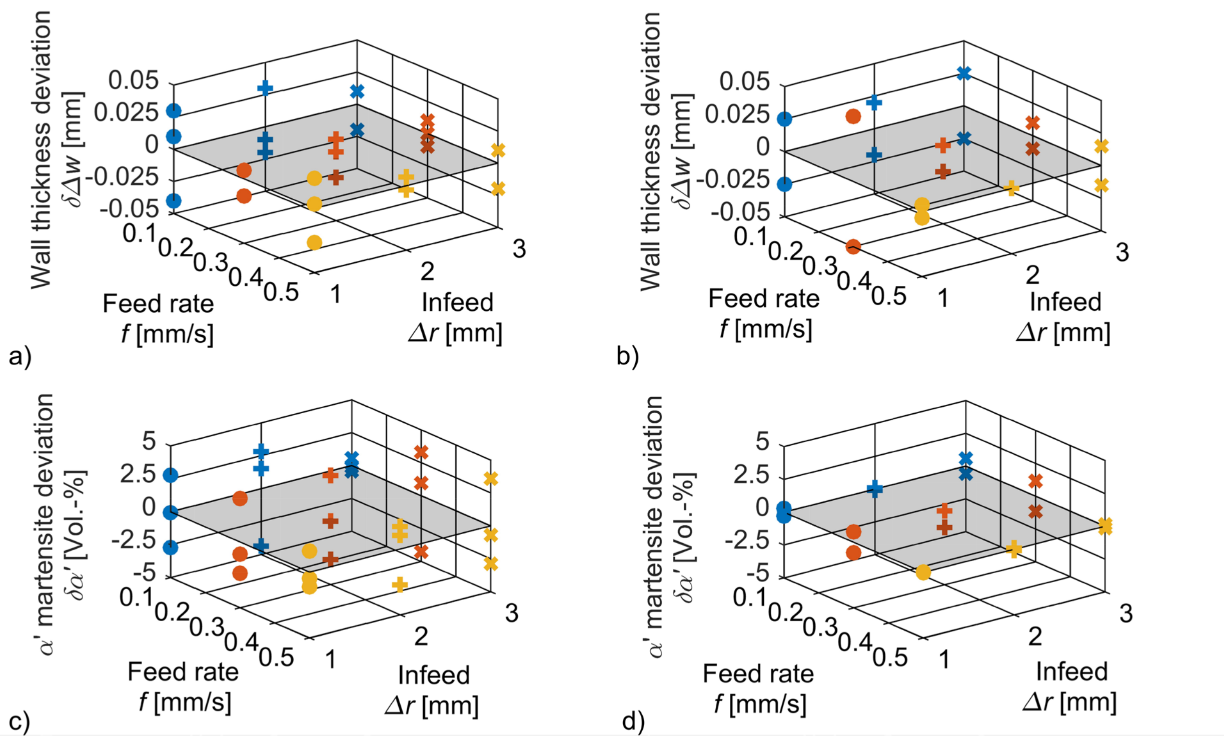

Fig. 7. Process deviations of the wall thickness reduction $\delta\Delta w$ and α'-martensite volume fraction $\delta\alpha'$ from the average values for Batch A (a+c) and Batch B (b+d) during repetitive experiments

According to the equation, there are three factors that have an impact on the calculated α'-martensite volume fraction: the feed rate and the wall thickness reduction acting as input quantities, as well as the model parameters c_1, c_2 and c_3 that describe the transfer behavior. However, while the feed rate is the same for each process parameter combination, the wall thickness reduction stochastically varies according to Fig. 7. It is analysed in the following how the uncertainty of wall thickness reduction leads to an uncertainty of the α'-martensite volume fraction by using the mathematical method of error propagation. According to [23], error propagation via a function $y = g(x_1, \ldots x_m)$ is described by Eq. 3

$$(\delta y)^2 = \sum_{i=1}^{m} \left(\frac{\partial g(x_1, \ldots x_m)}{\partial x_i} \right)^2 \Bigg|_0 (\delta x_i)^2, \tag{3}$$

where $\frac{\partial g(x_1,\ldots x_m)}{\partial x_i}$ denotes the partial derivative of function g for an arbitrary operating point, δx_i denotes the deviation of the system inputs $x_1 \ldots x_m$ and δy is the deviation of the system output. In most cases, for δx the standard deviation is chosen. However, Eq. 3 can be applied to an arbitrary deviation, if the deviation is sufficiently small. This restriction is caused by the fact that Eq. 3 is built on Taylor series expansion and linearization. In the following, the deviations from Fig. 7 are used that are in the range of the standard deviation. Thus, the equation can be applied.

For the analysis, it is additionally assumed that the model parameters are certain. In this case, the wall thickness reduction Δw is the only uncertain input δx_i and Eq. 3 is reduced to Eq. 4

$$\delta y = \frac{\partial g(x_1, \ldots x_m)}{\partial x_1} \Bigg|_0 \delta x_1. \tag{4}$$

More specifically, the deviation of the α'-martensite volume fraction $\delta\alpha'$ is calculated by the deviation of the wall thickness reduction $\delta\Delta w$ and the partial derivative of function g. In this case, function g is given by the material model equation 2 and the partial derivative (Eq. 5) is

$$\left.\frac{\partial g_\alpha}{\partial \Delta w}\right|_{\Delta w_0, f_0} = c_3\, c_1 \left(1 - e^{-\frac{[\varphi_r(\Delta w_0)]}{c_2}}\right) \cdot f_0^{c_3 - 1}. \tag{5}$$

Here, Δw_0 and f_0 denotes the nominal wall thickness reduction and the feed rate at the operating point, i.e. in case of uncertainty the mean values of Δw and f for multiple repetitions of specific process parameter combinations. This leads to Eq. 6 that describes the deviation of the α'-martensite volume fraction $\delta\alpha'$:

$$\delta\alpha'(\delta\Delta w, \Delta w_0, f_0) = c_3\, c_1 \left(1 - e^{-\frac{[\varphi_r(\Delta w_0)]}{c_2}}\right) \cdot f_0^{c_3 - 1} \cdot \delta\Delta w. \tag{6}$$

This equation can now be applied to the experimental results from Fig. 7a and b to estimate the impact of the wall thickness deviation $\delta\Delta w$ on the α'-martensite deviation. For this purpose, the deviation $\delta\Delta w$ from Fig. 7, the feed rate $f_0 = f$ related to those deviations and the measured mean wall thickness reduction $\Delta w_0 = \Delta w$ from Fig. 4 are inserted in Eq. 6 and the α'-martensite deviation $\delta\alpha'_{\text{prop}} = \delta\alpha'(\delta\Delta w, \Delta w_0, f_0)$ is calculated via propagation. The results are shown in Fig. 8 in comparison to the measured values α'_{meas} from the previous figure.

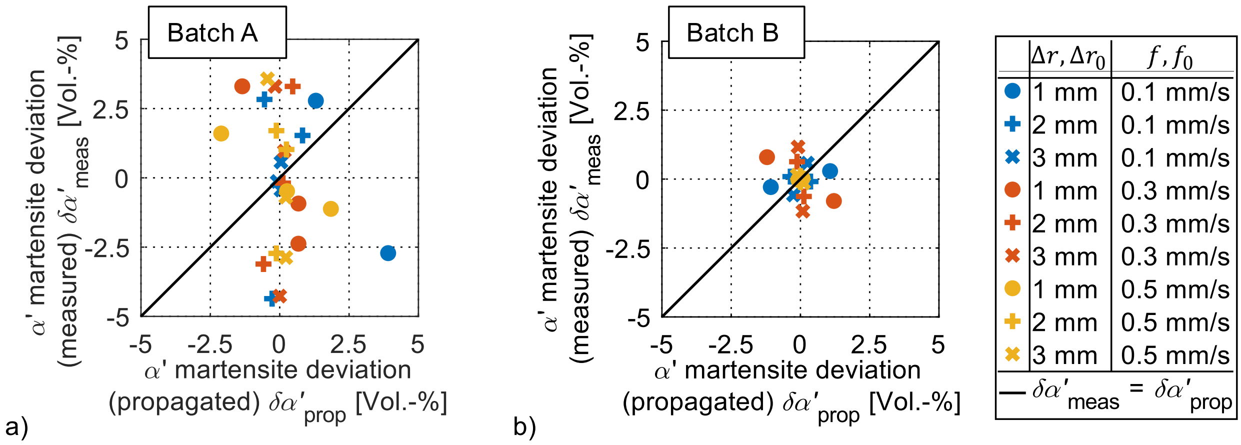

Fig. 8. Comparison between the α'-martensite deviations of each experiment $\delta\alpha'_{\text{meas}}$ from Fig. 7, measured via Feritscope, and the propagated α'-martensite deviations $\delta\alpha'_{\text{prop}}$, calculated from the wall thickness deviation δΔw, for Batch A (a) and Batch B

If all the measured α'-martensite deviations $\delta\alpha'_{\text{meas}}$ result from the uncertainty of the plastic deformation leading to $\delta\Delta w$, the quantities $\delta\alpha'_{\text{prop}}$ and $\delta\alpha'_{\text{meas}}$ would be equal. Thus, the data points in Fig. 8 would lay on the diagonal line that represents the equality of $\delta\alpha'_{\text{prop}}$ and $\delta\alpha'_{\text{meas}}$. However, it can be seen from Fig. 8a for Batch A that $\delta\alpha'_{\text{meas}}$ deviates from $\delta\alpha'_{\text{prop}}$ for most data points with a wide scatter in vertical direction of the plot. Thus, $\delta\alpha'_{\text{meas}}$ must be caused by another phenomenon. For Batch B, the results are more compact without the large scatter. However, also in this case the data points are not aligned along the diagonal.

It can be concluded that the deviation of the α'-martensite volume fraction does not result from the wall thickness reduction. Thus, there must be an uncertainty of the model parameters c_1, c_2 and c_3. From Table 2, it is already known that the material depicts a parametric uncertainty. In principle, a variation of the temperature may lead to a parametric uncertainty because α'-martensite is significantly influenced by the temperature (see [19, 20]). However, the experiments were performed with the same cooling as confirmed by additional measurement of the ambient and cooling temperature with minor variations of max. 3.5 °C, but those variations do not correlate the deviation of the α'-martensite. Therefore, the most probable explanation for the deviation of the α'-martensite are inhomogeneities of the material and fluctuations of the chemical composition within a batch. However, those variations within the batch are on a lower scale than the batch-to-batch variations.

Countering the Uncertainty by Closed-Loop Property Control

Nevertheless, both inner-batch and batch-to-batch variations are undesirable and should be reduced or minimized to produce workpieces of a specific quality. At this point, the usage of property control approaches from control engineering in context of flow forming could help to improve the flow forming of metastable. One possibility to counter the uncertainty is closed-loop property control. This type of control was proposed in [24] by Allwood et al. as a strategy to control metal forming processes. For the special case of flow forming of metastable austenite, the authors of the present paper already presented and validated a closed-loop property control approach in [25]. It consists of a control for the α'-martensite volume fraction (α'-martensite control) that is (optionally) extended by a control of the wall thickness reduction (wall thickness control) to ensure desired geometry while controlling the α'-martensite fraction. The general structure is shown in Fig. 9.

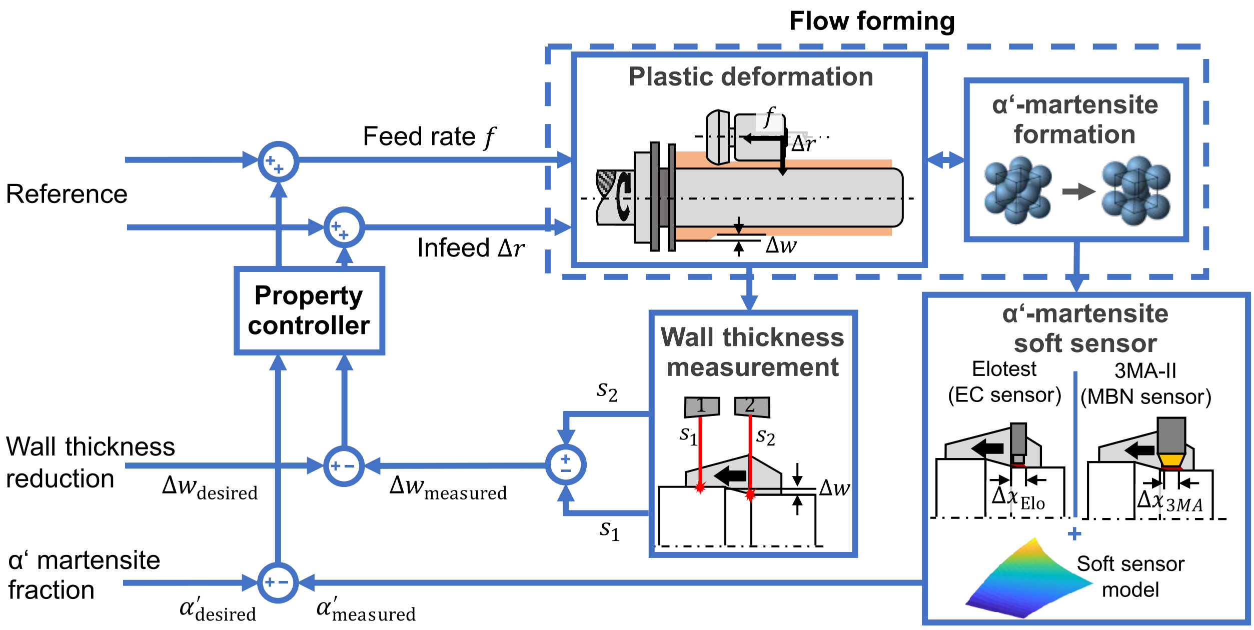

Fig. 9. Closed-loop property control structure for flow forming of metastable austenites

In the closed-loop control, the infeed Δr is corrected for setting the wall thickness reduction to a desired value and the feed rate f is utilized to achieve the desired α'-martensite volume fraction. For this purpose, the α'-martensite volume fraction is determined with a soft sensor approach since the Feritscope FMP30 is not suitable to detect the α'-martensite volume online during the workpiece production. For the soft sensor, micromagnetic measurements of the magnetic Barkhausen noise (MBN) with a 3MA-II sensor (Fraunhofer IZFP, Saarbruecken) or eddy current (EC) measurement by e.g. Elotest PL600 (Rohmann, Frankenthal) are used. Those sensors are placed at the machine support of the flow forming machine moving with the roller alongside the workpiece and measuring continuously in the already deformed workpiece area. There are also two laser distance sensors OM 70 (Baumer, Frauenfeld) mounted at the machine. One of the laser distance sensors is measuring in the deformed and the other in the undeformed area of the workpiece. From the difference of both sensor signals, the wall thickness reduction $\Delta w_{\text{measured}}$ is determined. Thus, online information about wall thickness reduction and the α'-martensite volume during flow forming is available as a feedback signal for the closed-loop control. Those feedback signals are further processed by a property controller. In the approach from [25], a PI controller is utilized for each control. The PI controller consists of a proportional and an integral gain. Both gains have a constant value that is predetermined by model-based control design methods offline before workpiece production with a real-time model of the flow forming process. The predetermined controller gains are then included into the flow forming machine control. Thus, they can be used online to calculate the correction signal to the feed rate f or the infeed Δr. This approach has already been successfully validated in [25]. However, it was not analyzed how the controller deals with the uncertainty in flow forming. This is investigated in the following for the α'-martensite control. For this purpose, a simulative study is performed using a real-time simulation model for flow forming of metastable austenites that was already proposed by the authors in [14, 26, 27]. In the study, multiple parts are manufactured closed-loop controlled with the same parameter combination while the α'-martensite formation is stochastically varied from part to part within range of the previously identified inner-batch fluctuations. Fig. 10 shows the result of the simulation study for Batch B. The aim was here to set the α'-martensite volume fraction to a desired value of 14 Vol.-%. This is achieved by consecutively reducing initial feed rate starting from $f = 0.25$ mm/s.

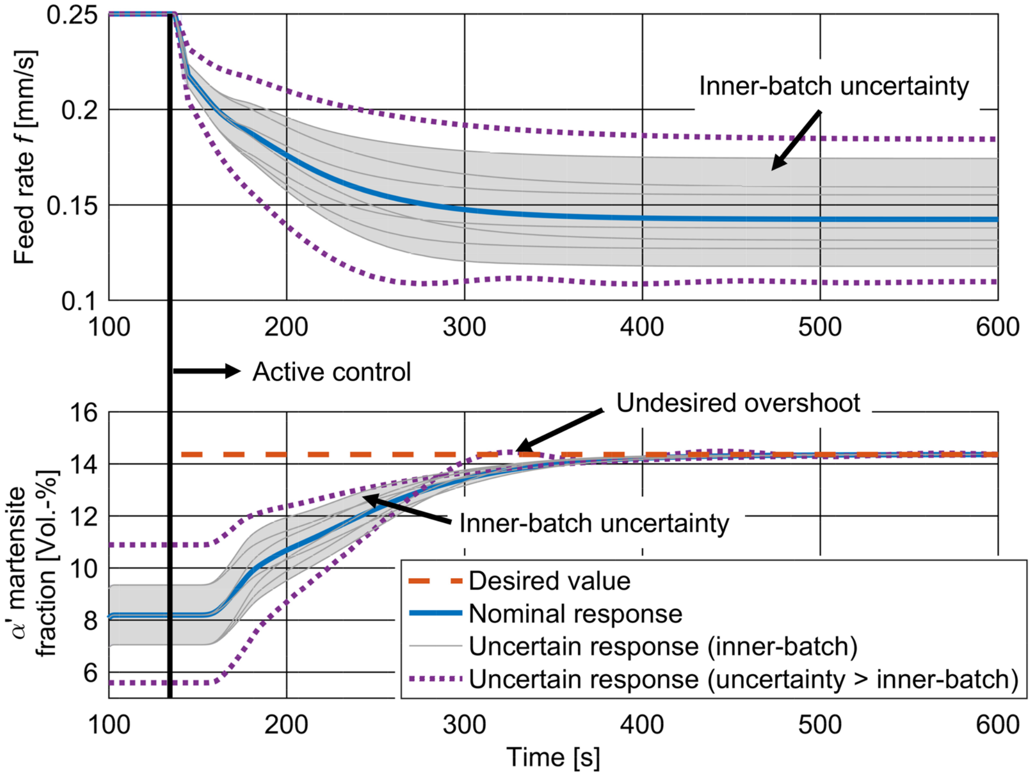

Fig. 10. Simulation result of the α'-martensite control for an uncertain α'-martensite phase transformation behavior (Batch B, Elotest soft sensor)

It can be seen from the measured α'-martensite volume fraction that the uncertainty leads to different initial values at the beginning that vary between 7.3 Vol.-% and 9.3 Vol.-%. Despite this variation, the desired value of 14 Vol.-% is finally reached in any case. This is possible since the controller corrects the feed rate f depending on the measurements to a value between 0.1315 mm/s and 0.1552 mm/s. Thus, the control reacts on the inner-batch variations. It can be stated that the uncertainty in the α'-martensite volume fraction leads to uncertainty in the feed rate f (both marked in grey in the figure), but the uncertainty concerning the α'-martensite formation within a batch is successfully compensated by the control. It is obvious that the control performance, i.e. the dynamics or the speed until reaching the desired value and the damping behavior of the control response, is also slightly affected by the uncertainty of α'-martensite formation. However, the impact of the uncertainty on the control performance is only minor if the uncertainty is within the range of the inner-batch variations. In the figure, there is also a simulation result where α'-martensite volume fraction at the beginning is 5.5 Vol.-%. It means that the deviation is outside of the inner-batch uncertainty, which may occur if the semifinished part belongs to another batch for example. In this case, the control reaction tends to overshoot, and if the deviation would be higher, the control becomes even unstable. Hence, the change to another batch depicts a limit for the constant-gain closed-loop property control.

It can be concluded that closed-loop property control with a constant gain is suitable to reduce the uncertainty within a batch. To handle the variety from batch to batch, it is necessary to retune the controller parameters. This could be done manually by identifying the transfer behavior or the parameters in Eq. 2 and applying the model-based control design methodology from [25] again for the new batch. However, this approach may be time consuming, as some workpieces for model identification must first be manufactured in an open-loop (without property control) before the actual workpieces with defined properties can be produced in the closed-loop control. Another possible solution is to adapt the controller parameters automatically. In this context, the closed-loop property control could be extended to an adaptive property control to automatically adapt the controller parameters concerning the batch-to-batch variations. The term adaptive control means that the controller parameters and / or the model for the determination of the controller parameters are automatically updated depending on the online measurements from the actual system. This type of control already exist in control engineering and the industry since the 1980's, but in the field of metal forming, an application of adaptive control in the sense of a closed-loop control adaption is only investigated in a few examples (see [28, 29]) until now. To extent the flow forming closed-loop property control, a suitable adaptation algorithm for PI controller is required. There are different types of adaption algorithms that can be divided in indirect methods, where a model is automatically updated and then the controller is systematically designed, and direct methods such as model reference adaptive control where the controller parameters are directly updated (see [30]). Such an approach could be adapted to flow forming to automatically counter the batch-to-batch uncertainty. In this case, the closed-loop property control would be extended by a closed-loop-controlled model and the measurements from the actual system would be continuously compared to the model. From the deviation between model and the actual system, the new controller parameters could be automatically calculated by a modified extended Kalman filter (MEKF, see [31]). However, this approach is not state of the art for flow forming and should be further investigated in future.

Summary

This paper focused on the uncertainty in flow forming of metastable austenites. Besides disturbance variables such as the temperature, this uncertainty especially results from the chemical composition and the initial wall thickness of the semifinished parts which differ from batch-to-batch and within a batch. It was found out that the uncertainty of the mean initial wall thickness leads to a small deviation of the resulting wall thickness reduction from part to part and does not significantly differ from batch to batch. However, it was evidenced that the α'-martensite formation shows a strong dependency on the material batch leading quantitively to a totally different transfer behavior. This effect could be interpreted as a parametric uncertainty. Additionally, there are also fluctuations in the experimental results within a batch that are directly related to the α'-martensite formation because they do not result from the uncertainty in plastic deformation as shown in the error propagation analysis. Thus, solutions are necessary to reduce the uncertainty from batch to batch and within a batch. It was shown that for the inner-batch fluctuations closed-loop property control is a suitable solution to reduce the uncertainty. To automatically counter batch-to-batch fluctuations, current research of the authors focuses on extending the existing closed-loop property control to an adaptive control that can adapt the controller parameters to an unknown material batch without additional experiments. Thus, the uncertainty in flow forming of metastable austenites could be reduced fully automatically in any case.

Acknowledgements

The authors would like to thank the German Research Foundation (Deutsche Forschungsgemeinschaft, DFG) for their support of the depicted research within the priority program SPP 2183 "Property-controlled metal forming processes", through project no. 424335026 "Property control during spinning of metastable austenites".

References

[1] A.E. Tekkaya, N. Ben Khalifa, G. Grzancic, R. Hölker, Forming of lightweight metal components: Need for new technologies, Procedia Engineering 81 (2014) 28–37. https://doi.org/10.1016/j.proeng.2014.09.125

[2] B. Arian, W. Homberg, L. Kersting, A. Trächtler, J. Rozo Vasquez, F. Walther, α'-martensite grading techniques in reverse flow forming of AISI 304L, Materials Research Proceedings (2024) 708–717. https://doi.org/10.21741/9781644903254-76

[3] B. Arian, W. Homberg, L. Kersting, A. Trächtler, J. Rozo Vasquez, F. Walther, Advanced thermomechanical flow forming: A novel approach to α' martensite control for enhanced material properties, Materials Research Proceedings (2025) 1167–1173. https://doi.org/10.21741/9781644903599-127

[4] B. Arian, W. Homberg, L. Kersting, A. Trächtler, J. Rozo Vasquez, F. Walther, Produktkennzeichnung durch lokal definierte Einstellung von ferromagnetischen Eigenschaften beim Drückwalzen von metastabilen Stahlwerkstoffen, in: G. Hirt (Ed.), 36. Aachener Stahlkolloquium – Umformtechnik "Ideen Form geben": 26.-27. October 2022, Eurogress Aachen, Tagungsband, Verlagshaus Mainz, Aachen, 2022, pp. 333–347

[5] A. Weidner, Deformation processes in TRIP/TWIP steels, Springer, Cham, 2020

[6] B.-A. Behrens, E. Doege, B. Springub, Transformation induced martensite evolution in metal forming processes of stainless steels, Steel Research International 75 (2004) 475–482. https://doi.org/10.1002/srin.200405799

[7] E. Wiens, W. Homberg, B. Arian, K. Möhring, F. Walther, Forming of parts with locally defined mechanical and ferromagnetic properties by flow-forming, in: G. Daehn, J. Cao, B. Kinsey, A.E. Tekkaya, A. Vivek, Y. Yoshida (Eds.), Forming the Future, Springer, Cham, 2021, pp. 1913–1924

[8] B.-A. Behrens, K. Brunotte, H. Wester, J. Peddinghausen, M. Till, Functionalisation of the boundary layer by deformation-induced martensite on bearing rings by means of bulk metal forming processes, in: METAL 2022 Conference proceedings 2022, pp. 250–255

[9] A. Weiß, W. Lehnert, H. Gutte, P.R. Scheller, Verbesserung der Kaltumformbarkeit austenitischer CrNi-Stähle durch Nutzung des Trip-Effektes, ATZ - Automobiltechnische Zeitschrift 107 (2005) 68–72. https://doi.org/10.1007/BF03221690

[10] M. Runge, Drücken und Drückwalzen: Umformtechnik, Werkstückgestaltung, Maschinen, Steuerungskonzepte, Verl. Moderne Industrie, Landsberg/Lech, 1993

[11] P.F. Pelz, P. Groche, M.E. Pfetsch, M. Schaeffner, Mastering uncertainty in mechanical engineering, Springer, Cham, 2021

[12] Deutsches Institut für Normung, Seamless steel tubes for pressure purposes - Technical delivery conditions - Part 5: Stainless steel tubes: German version EN 10216-5:2021, DIN Media, Berlin

[13] J. Talonen, P. Nenonen, G. Pape, H. Hänninen, Effect of strain tate on the strain-induced $\gamma \rightarrow \alpha'$-martensite transformation and mechanical properties of austenititc stainless steel, Metallurgical and Materials Transactions A (2005) 421–431. https://doi.org/10.1007/s11661-005-0313-y

[14] L. Kersting, B. Arian, J. Rozo Vasquez, A. Trächtler, W. Homberg, F. Walther, Innovative online measurement and modelling approach for property-controlled flow forming processes, Key Engineering Materials 926 (2022) 862–874. https://doi.org/10.4028/p-yp2hj3

[15] L. Kersting, S.R. Sander, B. Arian, J. Rozo Vasquez, A. Trächtler, W. Homberg, F. Walther, Improving the flow forming process by a novel closed-loop control, Materials Research Proceedings (2024) 1426–1435. https://doi.org/10.21741/9781644903131-158

[16] B. Podder, P. Banerjee, K.R. Kumar, N.B. Hui, Forward and reverse modelling of flow forming of solution annealed H30 aluminium tubes, Neural Computing and Applications 32 (2020) 2081–2093. https://doi.org/10.1007/s00521-018-3749-x

[17] J. Rozo Vasquez, L. Kersting, B. Arian, W. Homberg, A. Trächtler, F. Walther, Softsensor model of phase transformation during flow forming of metastable austenitic steel AISI 304L, in: J. Kusiak, Ł. Rauch, K. Regulski (Eds.), Numerical Methods in Industrial Forming Processes: Numiform 2023, Springer, Cham, 2024

[18] B. Arian, W. Homberg, J. Rozo Vasquez, F. Walther, M. Riepold, A. Trächtler, Forming of metastable austenitic stainless steel tubes with axially graded martensite content by flow-forming, ESAFORM 2021 (2021). https://doi.org/10.25518/esaform21.2759

[19] T. Angel, Formation of martensite in austenitic stainless steels: Effects of deformation, temperature, and composition, Journal of the Iron and Steel Institute 177 (1954) 165–174

[20] G.B. Olson, M. Cohen, Kinetics of strain-induced martensitic nucleation, Metallurgical and Materials Transactions A 6A (1975) 791–795

[21] M. Riepold, B. Arian, J. Rozo Vasquez, W. Homberg, F. Walther, A. Trächtler, Model approaches for closed-loop property control for flow forming, Advances in Industrial and Manufacturing Engineering 3 (2021). https://doi.org/10.1016/j.aime.2021.100057

[22] M. Smaga, F. Walther, D. Eifler, Investigation and modelling of the plasticity-induced martensite formation in metastable austenites, International Journal of Materials Research 97 (2006) 1648–1655. https://doi.org/10.3139/146.101396

[23] F.A. Seiler, Error propagation for large errors, Risk Analysis 7 (1987) 509-518. https://doi.org/10.1111/j.1539-6924.1987.tb00487.x

[24] J.M. Allwood, S.R. Duncan, J. Cao, P. Groche, G. Hirt, B. Kinsey, T. Kuboki, M. Liewald, A. Sterzing, A.E. Tekkaya, Closed-loop control of product properties in metal forming, CIRP Annals 65 (2016) 573–596. https://doi.org/10.1016/j.cirp.2016.06.002

[25] L. Kersting, B. Arian, J. Rozo Vasquez, A. Trächtler, W. Homberg, F. Walther, Modellbasierter Entwurf und Validierung einer Eigenschaftsregelung für das Drückwalzen metastabiler Austenite, at - Automatisierungstechnik 73 (2025) 527–540. https://doi.org/10.1515/auto-2024-0127

[26] L. Kersting, B. Arian, J. Rozo Vasquez, A. Trächtler, W. Homberg, F. Walther, Echtzeitfähige Modellierung eines innovativen Drückwalzprozesses für die eigenschaftsgeregelte Bauteilfertigung, at - Automatisierungstechnik 71 (2023) 68–81.https://doi.org/10.1515/auto-2022-0106

[27] L. Kersting, B. Arian, J. Rozo Vasquez, A. Trächtler, W. Homberg, F. Walther, State-space modelling approach for control and observer design in property-controlled reverse flow forming, IFAC-PapersOnLine 59 (2025) 109–114. https://doi.org/10.1016/j.ifacol.2025.03.020

[28] C. Schulte, X. Li, D. Abel, G. Hirt, Model-based control of the strip roughness in cold rolling, IFAC-PapersOnLine 54 (2021) 109–114. https://doi.org/10.1016/j.ifacol.2021.10.059

[29] Y. Lim, R. Venugopal, A. Galip Ulsoy, Auto-tuning and adaptive control of sheet metal forming, Control Engineering Practice 20 (2012) 156–164. https://doi.org/10.1016/j.conengprac.2011.10.006

[30] K.J. Åström, T. Hägglund, C.C. Hang, W.K. Ho, Automatic tuning and adaptation for PID controllers - a survey, Control Engineering Practice 1 (1993) 699-714. https://doi.org/10.1016/0967-0661(93)91394-C

[31] A. Alessandri, M. Cuneo, S. Pagnan, M. Sanguineti, A recursive algorithm for nonlinear least-squares problems, Computational Optimization and Applications 38 (2007) 195–216. https://doi.org/10.1007/s10589-007-9047-7